Chemical Vapor Sensing with Mono layer MoS2

6 AUTHORS, INCLUDING:

Adam Friedman
United States Naval Research Laboratory
55 PUBLICATIONS **783** CITATIONS

SEE PROFILE

Enrique Cobas
United States Naval Research Laboratory
22 PUBLICATIONS **1,438** CITATIONS

SEE PROFILE

Paul M. Campbell
United States Naval Research Laboratory
85 PUBLICATIONS **3,916** CITATIONS

SEE PROFILE

Berend T Jonker
United States Naval Research Laboratory
**345** PUBLICATIONS **7,339** CITATIONS

SEE PROFILE

Chemical Vapor Sensing with Monolayer MoS₂

F. K. Perkins,*[,†] A. L. Friedman,[†] E. Cobas,[‡] P. M. Campbell, G. G. Jernigan, and B. T. Jonker*

Naval Research Laboratory, Washington, District of Columbia 20375, United States

S *Supporting Information*

ABSTRACT: Two-dimensional materials such as graphene show great potential for future nanoscale electronic devices. The high surface-to-volume ratio is a natural asset for applications such as chemical sensing, where perturbations to the surface resulting in charge redistribution are readily manifested in the transport characteristics. Here we show that single monolayer MoS₂ functions effectively as a chemical sensor, exhibiting highly selective reactivity to a range of analytes and providing sensitive transduction of transient surface physisorption events to the conductance of the monolayer channel. We find strong response upon exposure to triethylamine, a decomposition product of the V-series nerve gas agents. We discuss these results in the context of analyte/sensor interaction in which the analyte serves as either an electron donor or acceptor, producing a temporary charge perturbation of the sensor material. We find highly selective response to electron donors and little response to electron acceptors, consistent with the weak *n*-type character of our MoS₂. The MoS₂ sensor exhibits a much higher selectivity than carbon nanotube-based sensors.

KEYWORDS: *Chemical sensor, MoS₂, molybdenum disulfide, two-dimensional materials, vapor sensing*
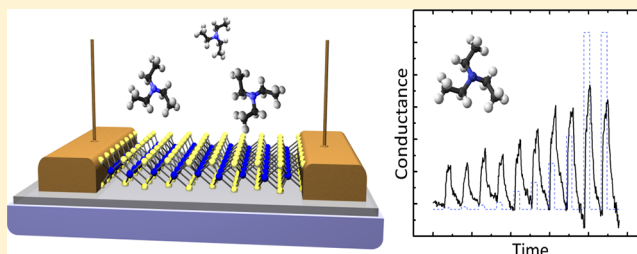
The planar habit of two-dimensional (2D) materials is attractive for the ultimate size scaling envisioned by Moore's Law and beyond[1,2] and offers relative ease of fabrication, the requisite large-scale integration, and exceedingly low power consumption. The very high surface-to-volume ratio of such single or few monolayer materials enables highly efficient gating of charge transport via surface gates, obviating the need for the more complex growth and fabrication procedures required for wrapped-gate nanowire transistors.

Graphene has captivated attention since the first measurements of high mobility transport were reported in single layer flakes.[3] Progress toward monolithic graphene circuits was recently demonstrated by the fabrication of wafer-scale inductor/transistor circuits,[4] vertically integrated graphene/graphite transistor arrays,[5] and transistors with improved on/off ratios.[6] Recent effort has focused on other 2D materials such as the transition metal dichalcogenides, and field effect transistors with a monolayer of MoS₂ as the active channel were shown to exhibit high on/off ratios at room temperature, ultralow standby power dissipation, and well-defined photoresponse.[7−9] Very recent work has demonstrated fabrication of complex integrated logic circuits based on bilayer MoS₂ transistors,[10] and significant advances have been made in large area growth of MoS₂ on several substrates.[11−13]

The high surface-to-volume ratio is also important for new sensor materials which must exhibit selective reactivity upon exposure to a range of analytes (determined by the character of surface physisorption sites), rapid response and recovery, and sensitive transduction of the perturbation to the output parameter measured. The conductivity of graphene near the charge neutrality point has been shown to change with adsorption of a variety of analytes, but annealing to 150 °C was required to restore the conductivity to its original value, suggesting the analytes were strongly bound.[14] Other work has shown that graphene's intrinsic response to physisorption of analytes such as ammonia is very small.[15] The sensitivity can be enhanced by functionalizing the graphene surface, for example, by oxidation,[16] but these devices showed little selectivity, and functionalization introduces additional complexity to the fabrication process. Recent work has shown that the selectivity of graphene sensors can be enhanced by measuring analyte-dependent changes in the low frequency noise spectrum, although degassing in vacuum at room temperature for several hours between measurements was needed to obtain good reproducibility.[17] Other 2D materials are likely to offer selective surface reactivity to physisorbed species, and if semiconducting in character, can provide both lower background carrier densities and the possibility of photomodulated sensing mechanisms.

We have fabricated planar sensor structures consisting of a monolayer MoS₂ channel on SiO₂/Si wafers, as shown in Figure 1a and b. The change in channel conductance was measured during exposure to a variety of analytes, including standard laboratory chemicals, solvents, and simulants/byproducts for explosives, nerve agents, or precursors thereof. The conductance increases rapidly with exposure to triethylamine (TEA, a decomposition product of the V-series of nerve gas agents) and acetone, and is unaffected by exposure to many
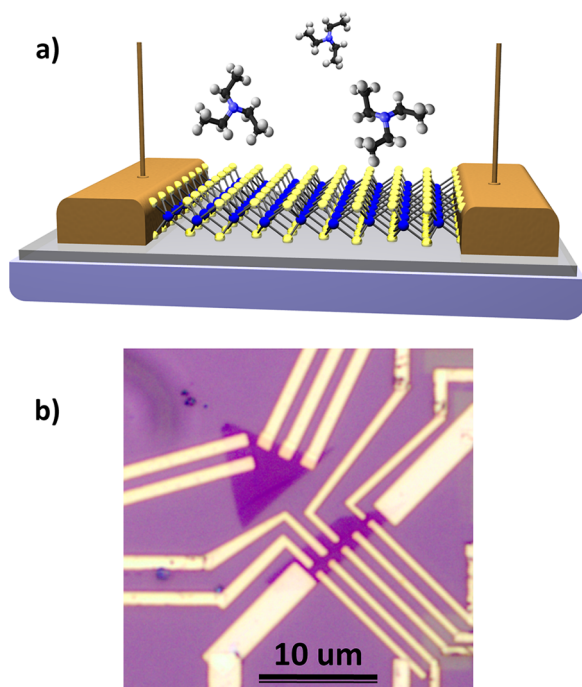
Figure 1. Schematic and image of the MoS_2 monolayer sensor. (a) A single monolayer of MoS_2 is supported on an SiO_2/Si substrate and contacted with Au contact pads. Transient physisorption of molecules induces temporary changes in the conductivity of the monolayer channel. (b) An optical image of the processed devices showing the monolayer MoS_2 flakes electrically contacted by multiple Au leads.

other analytes or gases, including dichlorobenzene, dichloropentane, nitromethane, nitrotoluene, and water vapor. We directly compare the MoS_2 sensor response with that of similar planar sensors fabricated from monolayer graphene and carbon nanotube networks, and from these data obtain consistent evidence for a charge transfer mechanism involving transient doping of the sensor channel.

MoS_2 is a layered compound with weak interaction between the layers, similar to graphite, and is widely used as a lubricant. Each layer consists of a plane of molybdenum atoms sandwiched between layers of sulfur atoms (Figure 1a). It is relatively nonreactive at moderate temperatures (<350 °C)—it is difficult to oxidize and unaffected by dilute acids. In contrast with graphite/graphene, it is a semiconductor with an indirect bandgap (~1.2 eV) and exhibits catalytic properties useful for hydrodesulfurization.[18] Recent work has shown that a single monolayer of MoS_2 exhibits properties markedly different from the bulk: it transitions from an indirect to direct gap semiconductor (~1.9 eV) with high luminescence efficiency[19,20] and can be used as the transport channel in a field effect transistor with high on/off ratio[7] and pronounced photoresponse.[8,9] The resistivity of exfoliated MoS_2 flakes 2–4 layers thick was shown to slowly increase (over 30 s) upon exposure to NO molecules followed by a 2 min approach to saturation, attributed to strong chemisorption, with a similarly slow decrease when the NO was removed.[21] The behavior of single monolayer MoS_2 showed an unstable response.[21]

Our sensor devices were fabricated from monolayer flakes of MoS_2 that were exfoliated from bulk samples using the "Scotch tape" method and deposited onto a 270 nm thick thermal SiO_2 film on Si wafers. Electrical contacts were placed on the MoS_2 flake by liftoff processes using electron beam lithography

followed by electron beam evaporation of Au and Ti/Au. An image of a typical sensor device is shown in Figure 1b. The bulk samples were obtained from three different sources, and the responsivity of the sensor flakes showed some variability that we attribute to variations in the purity of the original bulk samples. Further details appear in the Methods section and the Supporting Information file.

The electrical response to vapor exposure of a selected analyte was evaluated in a combined probe station/gas bubbler dosing system described elsewhere.[22] The gas flow, analyte concentration, and analyte pulse sequence are controlled by computer via appropriate mass flow controllers and valves. The analyte concentration is recorded as a percent of its equilibrium vapor pressure at 20 °C, P_0. The sample conductivity is continuously measured using standard lock-in amplifier techniques while a timed sequence of analyte pulses of selected concentration are introduced into the 5 lpm N_2 carrier gas stream. The data are presented as a change in conductivity, $\Delta G/G_0$, versus time, where G_0 is the initial conductivity when the pulse sequence is begun. All data are obtained at room temperature and ambient pressure.

The sensor response was measured for a variety of analytes, including those considered to be electron donors, acceptors, or highly polar molecules. The MoS_2 monolayer sensor exhibits a pronounced response to triethylamine (TEA−$N(CH_2−CH_3)_3$) exposure, a laboratory-safe decomposition product from the V-series nerve gas agents. The response to a sequence of 10 TEA pulses, each with a concentration of 0.002% P_0 (~1 ppm), is shown in Figure 2a. The timing of the pulse sequence is shown as a dashed line—the TEA is on for 15 s and off for 30 s (within the constant 5 lpm N_2 carrier flow). Upon exposure to TEA, the MoS_2 conductivity increases abruptly, with an initially rapid rise (~5 s) followed by a slower approach to saturation. This initial response is much more rapid than the 30 s reported previously for multilayer MoS_2.[21] Single pulse measurements at 0.02% P_0 (10 ppm) show that the response saturates at exposure times of ~60 s for this concentration. When the TEA is valved off, the conductivity shows the reverse behavior, with an initially rapid 5 s decrease and a slower approach to baseline. These sawtooth responses are superposed on a monotonically increasing background, which we tentatively attribute to charge accumulation.

A control measurement with no TEA in the pulsed gas sequence exhibits no change in conductivity (red curve), confirming that the observed response is due to interaction of the MoS_2 with TEA and not to changes in gas flow or residual contaminants in the N_2 carrier gas or in the plumbing of the dosing system. A second control measurement showed that the monolayer MoS_2 sensor (green curve) exhibited no response to water vapor (0.025% P_0 ~ 6 ppm), a desirable characteristic, while a monolayer graphene sensor (purple curve) shows a pronounced response to this ubiquitous background constituent.

The amplitude of the conductivity change increases with increasing TEA concentration. Figure 2b shows the device response to a sequence of pulses in which the TEA concentration increases from 0.002% P_0 (1 ppm) to 0.2% P_0 (100 ppm) over a total pulse sequence of 450 s. The conductivity change with each TEA pulse exhibits similar characteristics as noted above, with an initially rapid rise and fall and a positively sloped background (removed in the figure). The dependence of the change in conductivity on TEA concentration is summarized in Figure 2c, and the error bars
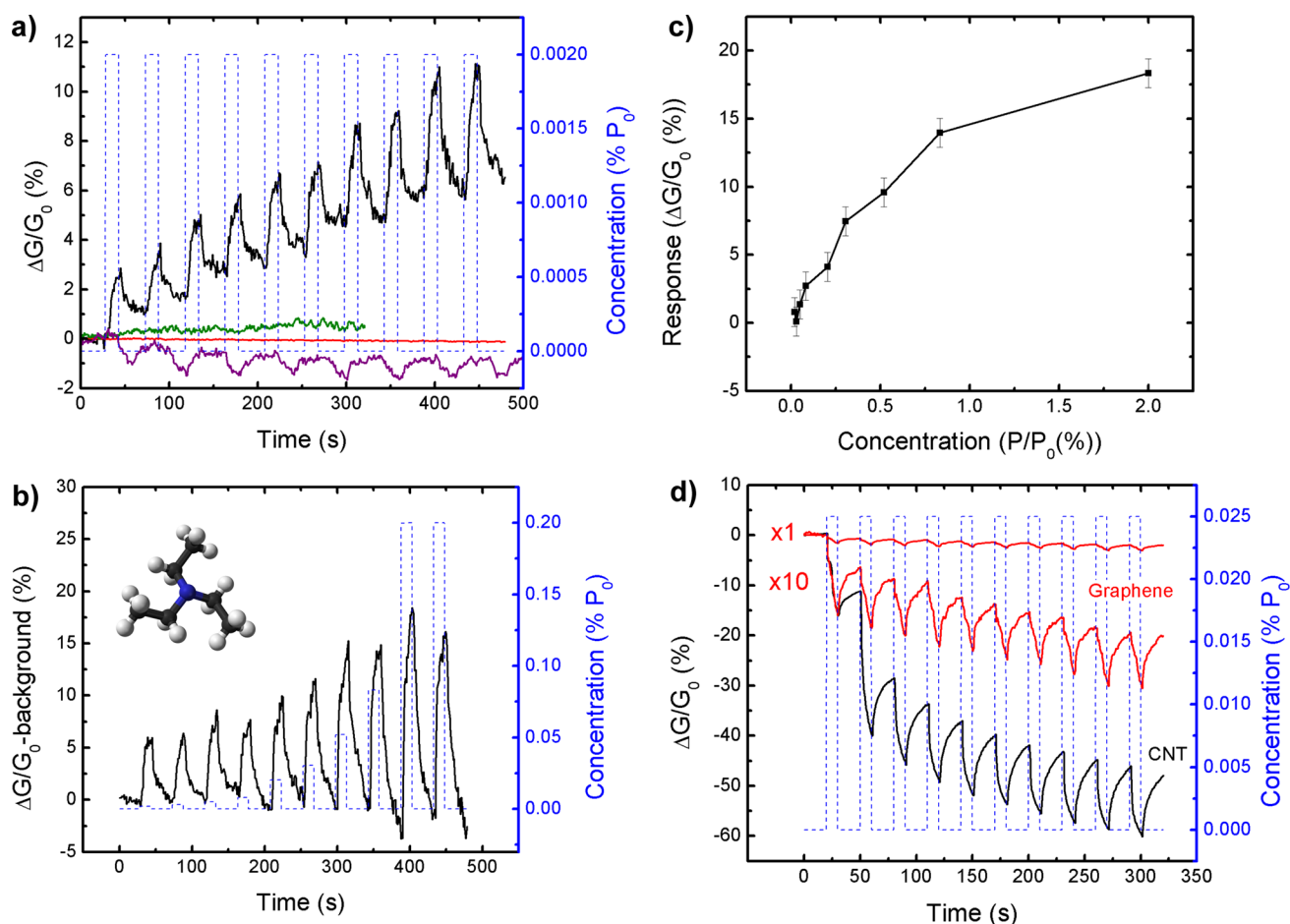
Figure 2. Response of sensors to triethylamine (TEA) exposure. (a) Change in conductivity of the monolayer MoS_2 sensor channel upon exposure to a sequence of 0.002% P_0 TEA pulses (black line). The dashed blue lines show the pulse timing (15 s on/30 s off) and concentration. The solid red line shows the response to exposure of nitrogen only and serves as a control experiment. The solid green and purple lines show the response of the MoS_2 and graphene sensors to water vapor pulses (0.025% P_0), respectively. (b) Same as part a, but for a series of exposure pulses in which the TEA concentration increases from 0.002% P_0 to 0.2% P_0. A positive slope background has been removed. The inset shows a model of the TEA molecule, in which the nitrogen atom is blue, the carbon atoms are black, and the hydrogen atoms are light gray. (c) The amplitude of the conductivity change increases with TEA concentration. The vertical axis is the response to each individual pulse (not the time integrated response). (d) Change in conductivity of a CVD graphene monolayer (red) and CNT-network sensor (black) upon exposure to a sequence of 0.025% P_0 TEA pulses (10 s on/20 s off).

illustrate the differences in relative sensitivity observed. These differences could not simply be attributed to geometric factors, but we cannot exclude variations in inadvertent residual contamination during device fabrication. The strong response and excellent signal-to-noise provide a TEA detection threshold of 10 ppb.

For comparison, similar data were acquired for planar sensors fabricated from (a) monolayer graphene grown by chemical vapor deposition on copper and (b) a carbon nanotube (CNT) network consisting of a dense array of CNTs forming an electrically continuous thin film, as the transport/sensor channel. These data are shown in Figure 2d, where $\Delta G/G_0$ is plotted for a sequence of TEA pulses (10s on, 20 s off) of 0.025% P_0 (12 ppm) concentration. The CNT response amplitude to a single pulse is comparable to that of the MoS_2 monolayer, while that of the graphene sensor is much smaller. However, in marked contrast with the response exhibited by the MoS_2, the graphene and CNT conductivity both *decrease* with TEA exposure, and the data are superposed on a negatively sloped background.

The opposite response of the MoS_2 and graphene/CNT sensors can be understood to first order by considering the transient charge perturbation to the sensor material upon interaction with the TEA molecule. Our MoS_2 monolayer samples are *n*-type, while the air-exposed CNT networks exhibit a *p*-type character,[23] and the graphene device as fabricated possesses a Dirac point at a substantial positive substrate bias indicating that the dominant carriers are holes. TEA is a strong electron donor, and thus transient physisorption will enhance the majority carrier density and conductivity for MoS_2 but decreases these parameters on graphene and the CNT network. The opposite response of the MoS_2 and graphene/CNT devices to TEA exposure provides a strong indicator of TEA presence with high confidence. In the following paragraphs, we make comparison to the CNT network devices, because they have been shown to be highly sensitive to a wide variety of analytes.[23,24]

The response of the MoS_2 sensor to analytes considered to be weak donors was correspondingly weaker. For example, exposure to tetrahydrofuran, $(CH_2)_4O$, produced only a modest response (<10% of that shown in Figure 2a), while

exposure to dimethylformamide, $(CH_3)_2NC(O)H$, produced no response above the noise level.

The response and sensitivity of the MoS_2 monolayer to other classes of analytes was determined in a similar fashion. The response to a pulse sequence of acetone $(CH_3)_2CO$, a highly polar molecule, is shown in Figure 3a, where the acetone
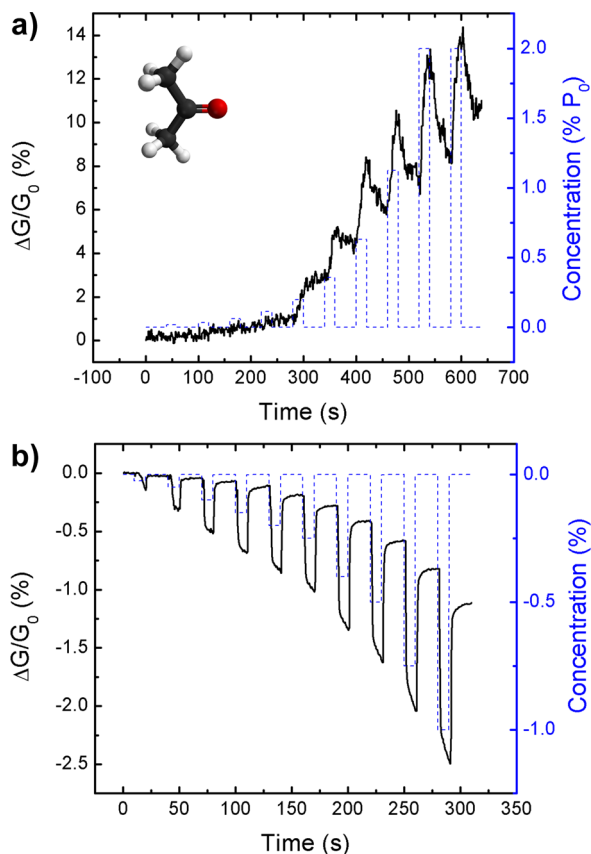

Figure 3. Response of sensors to acetone. (a) Change in conductivity of the monolayer MoS_2 sensor channel upon exposure to a sequence of pulses in which the acetone concentration increases from 0.02% P_0 to 2% P_0 (black line). The dashed blue lines show the pulse timing (20 s on/40 s off) and concentration. (b) Same as part a, but for a CNT-network sensor, and the acetone concentration increases from 0.01% P_0 to 1% P_0 with a pulse sequence of 10 s on/20 s off. The inset shows a model of the acetone molecule, in which the oxygen atom is red, the carbon atoms are black, and the hydrogen atoms are light gray.

concentration increases from 0.02% P_0 (50 ppm) to 2% P_0 (5000 ppm). The conductivity again increases upon exposure, with temporal characteristics similar to those observed for TEA—the incremental change in conductivity is strongly correlated with the exposure pulse sequence, the amplitude of $\Delta G/G_0$ is comparable for a given concentration, and the background exhibits a positive slope over the total duration of the exposure. The sensitivity to acetone is much lower than for TEA, with a detection threshold of ~500 ppm. The corresponding response of a CNT network sensor is shown in Figure 3b and exhibits a complementary response consistent with the transient charge perturbation model discussed above: the incremental conductivity decreases with acetone exposure, and the background exhibits a negative slope.

In contrast with the relatively strong responses described above, the MoS_2 sensor exhibited no measurable change in conductivity upon exposure to analytes considered to be

electron acceptors, including o-dichlorobenzene, 1,5-dichloropentane, o-nitrotoluene, and nitromethane at concentrations as high as 2% P_0 (P_0 = 1350, 960, 136, and 37 400 ppm, respectively), although the CNT devices respond to all. We note, however, that transport in CNTs is also affected by dipole-induced scattering,[25] a mechanism that would only decrease conductivity, and may not be relevant for 2D materials such as MoS_2. Thus the MoS_2 sensor exhibits a much higher degree of selectivity than the CNT-based sensors, a desirable sensor characteristic. As an example, the response to a sequence of nitrotoluene (NT) pulses, a laboratory-safe simulant for the explosive trinitrotoluene (TNT), is shown in Figure 4. As the
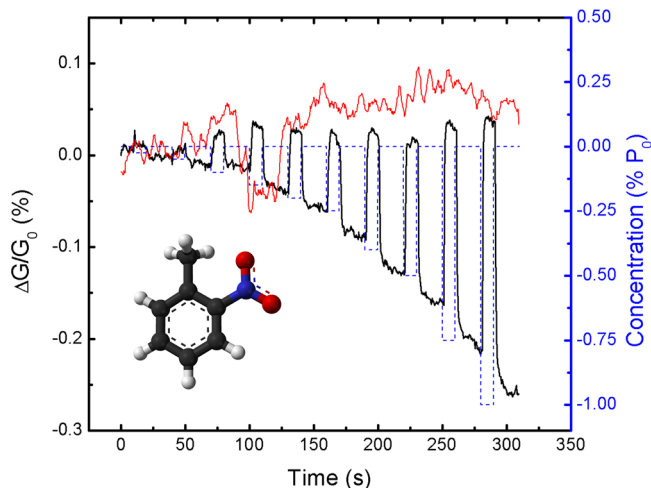

Figure 4. Response of sensors to nitrotoluene. The monolayer MoS_2 sensor (red line) shows no response to analytes such as nitrotoluene which tend to act as acceptors, while the CNT-network sensor (black line) shows a pronounced response. The nitrotoluene concentration increases from 0.01% P_0 to 1% P_0 and is shown inverted for convenience to facilitate comparison with the sensor response. The pulse sequence is 10 s on/20 s off. The inset shows a model of the nitrotoluene molecule, in which the nitrogen atom is blue, the oxygen atoms are red, the carbon atoms are black, and the hydrogen atoms are light gray.

NT concentration increases from 0.01% P_0 to 1% P_0, no change in conductivity of the MoS_2 monolayer is visible. The corresponding response of the CNT network sensor is shown for comparison, with the CNT conductivity increasing significantly upon exposure.

A histogram summarizing the sensitivity and selectivity of both the monolayer MoS_2 and CNT network sensors to these various analytes appears in Figure 5. The MoS_2 monolayer sensor displays good sensitivity, high selectivity, and a response that is typically opposite in polarity to that of CNT networks. While the states responsible for the MoS_2 in-plane conductivity derive from the sulfur−molybdenum hybridized orbitals, we hypothesize that the interaction mechanism with the analyte is mediated by the localized lone pair orbitals of the sulfur end units. Zonnevylle et al. modeled the atomic orbital configuration for planar MoS_2 sheets to understand the process of hydrodesulfurization.[26] They found that the Mo $3d_{xy}$ orbitals are used to form the Mo−S bond. The Mo $3d_{yz}$ orbitals and S $2p$ orbitals extend above the surface plane and are free to interact—the charge density distributions make the Mo $3d_{yz}$ slightly reduced (negatively charged) and the S $2p$ slightly oxidized (positively charged). It is this polarized surface that
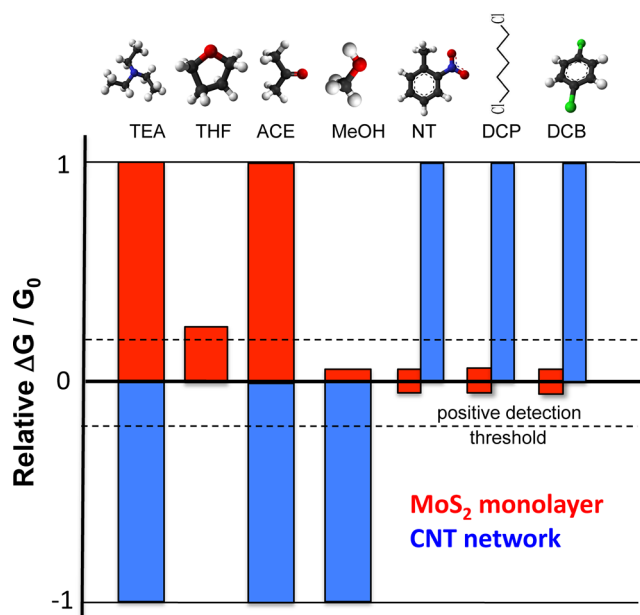
Figure 5. Histogram of MoS_2 and CNT-network sensor responses to various analytes. A qualitative summary of the response of the sensors to the analytes tested. The responses are broadly categorized as high, low, or null. The MoS_2 sensor exhibits a much higher selectivity and a complementary response to the CNT-network sensor. The analytes from left to right are triethylamine (TEA), tetrahydrofuran (THF), acetone, methanol, nitrotoluene (NT), 1,5-dichloropentane (DCP), and 1,4-dichlorobenzene (DCB). Ball-and-stick models of the analyte molecules are shown, in which nitrogen atoms are blue, oxygen atoms are red, carbon atoms are black, chlorine atoms are green, and hydrogen atoms are light gray.

attracts the other plane of MoS_2 in the bulk layered structure. We suspect that the SiO_2 substrate (known for its own positive charge) supporting the monolayer of MoS_2 compensates the negative charge of the Mo $3d_{yz}$ orbitals, leaving only the positively charged S available for gas/surface interactions. Thus the MoS_2 sheet tends to interact strongly with donor-like analytes, consistent with our experimental observations. Exposure to a wider range of analytes will provide further insight into the selectivity and response mechanisms.

Other 2D materials (TaS_2, WSe_2, $NbSe_2$, MgB_2, BN, etc.) are likely to offer complementary sensitivity due to different chemical composition and bonding. We envision development of suites of these 2D material sensors and carbon nanotubes with complementary responsivies, integrated with transistor amplifiers fabricated from the same materials, enabling unambiguous identification of a wide range of analytes in a very compact and low power package.

Methods. Planar devices were fabricated from MoS_2 exfoliated monolayer flakes using the "Scotch tape" method deposited onto a 270 nm thermal SiO_2 film on n-type Si wafers. Optical contrast and Raman spectroscopy were used to identify and confirm the monolayer areas used for subsequent processing. After optical inspection of the wafers in a microscope and isolation of suspected monolayers, atomic force microscopy measurements were performed to ensure accurate monolayer selection (1 ML ∼ 0.7 nm). Raman data and photoluminescence spectra analysis also confirm that the samples were single monolayer.[20,27] Ti/Au bond-pad contacts were formed by e-beam lithography using MMA/PMMA resist and metal evaporation and lift-off in acetone. A second e-beam

lithography step/metal evaporation/lift-off is performed to connect the MoS_2 to the bond pads with an Au contact line. Excess MoS_2 near the device is removed by defining a mesa level with another electron beam lithography step and then reactive ion etching in SF_6/O_2.

A combined electrical probe station−gas bubbler system[22] was used to determine the electrical response of the sensor samples to controlled exposures of various analytes. Briefly, dry N_2 is bubbled at low flow rates (milliliters per minute) by means of a glass frit through a container of liquid analyte with an equilibrium vapor pressure P_0 (at 20 °C).[28] It is expected that the N_2 stream leaving the bubbler is saturated with analyte vapor. This vapor stream is diluted by mixing with a constant flow of 200 mlpm dry N_2. Actual concentration of analyte is checked in a residual gas analyzer equipped with a capillary and differential pumping to achieve operation at atmospheric pressure (Hiden Analytical Inc. HPR-20 QIC). This diluted vapor stream is switched into a much larger 5 lpm N_2 flow by means of a solenoid-activated valve to create a gas of controlled high dilution. This gas stream is directed at the sample under test from a separation of a few millimeters.

Electrical contact to the sample pads is provided through Au-coated tungsten probe tips, and the conductivity between two contacts on the MoS_2 is measured by applying a small AC voltage (∼100 mVAC RMS, 1 kHz) to one electrode while observing the voltage drop across a bias resistor between another electrode and ground with a lock-in amplifier. The value of the bias resistor is selected to approximately match the nominal impedance of the MoS_2 channel. In this way we can measure resistance with a high signal-to-noise ratio.

ASSOCIATED CONTENT

Ⓢ Supporting Information

Description of the sample fabrication and measurements. This material is available free of charge via the Internet at http://pubs.acs.org.

AUTHOR INFORMATION

Corresponding Author

*E-mail: keith.perkins@nrl.navy.mil, berry.jonker@nrl.navy.mil.

Author Contributions

†These authors contributed equally.

Notes

The authors declare no competing financial interest.
‡NRL Karle Fellow.

■ REFERENCES

(1) Geim, A. K.; Novoselov, K. S. The Rise of Graphene. *Nat. Mater.* **2007**, *6*, 183−191.

(2) *International Technology Roadmap for Semiconductors (ITRS)*; Semiconductor Industry Association: Austin, TX, 2011; http://www.itrs.net.

(3) Novoselov, K. S.; Geim, A. K.; Morozov, S. V.; Jiang, D.; Zhang, Y.; Dubonos, S. V.; Griorieva, I. V.; Firsov, A. A. Electric Field Effect in Atomically Thin Carbon Films. *Science* **2004**, *306* (5696), 666−669.

(4) Lin, Y.-M.; Valdes-Garcia, A.; Han, S.-J.; Farmer, D. B.; Meric, I.; Sun, Y.; Wu, Y.; Dimitrakopoulos, C.; Grill, A.; Avouris, P.; Jenkins, K. A. Wafer scale graphene integrated circuit. *Science* **2011**, *332*, 1294−1297.

(5) Park, J.-U.; Nam, S.; Lee, M.-S.; Lieber, C. M. Synthesis of monolithic graphene-graphite integrated electronics. *Nat. Mater.* **2011**, *11*, 120−125.

(6) Xia, F.; Farmer, D. B.; Lin, Y.-M.; Avouris, P. Graphene field-effect transistors with high on/off current ratio and large transport band gap at room temperature. *Nano Lett.* **2010**, *10*, 715−718.

(7) Radisavljevic, B.; Radenovic, A.; Brivio, J.; Giacometti, V.; Kis, A. Single-layer MoS_2 transistors. *Nat. Nanotechnol.* **2011**, *6*, 147−150.

(8) Yin, Z.; Li, H.; Li, H.; Jiang, L.; Shi, Y.; Sun, Y.; Lu, G.; Zhang, Q.; Chen, X.; Zhang, H. Single layer MoS_2 phototransistors. *ACS Nano* **2012**, *6*, 74−80.

(9) Lee, H. S.; Min, S.-W.; Chang, Y.-G.; Park, M. K.; Nam, T.; Kim, H.; Kim, J. H.; Ryu, S.; Im, S. MoS_2 nanosheet phototransistors with thickness-modulated optical energy gap. *Nano Lett.* **2012**, *12*, 3695−3700.

(10) Wang, H.; Yu, L.; Lee, Y.-H.; Shi, Y.; Hsu, A.; Chin, M. L.; Li, L.-J.; Dubey, M.; Kong, J.; Palacios, T. Integrated circuits based on bilayer MoS_2 transistors. *Nano Lett.* **2012**, *12*, 4674−4680.

(11) Liu, K.-K.; Zhang, W.; Lee, Y.-H.; Lin, Y.-C.; Chang, M.-T.; Su, C.-Y.; Chang, C.-S.; Li, H.; Shi, Y.; Zhang, H.; Lai, C.-S.; Li, L.-J. Growth of Large-Area and Highly Crystalline MoS_2 Thin Layers. *Nano Lett.* **2012**, *12*, 1538−1544.

(12) Shi, Y.; Zhou, W.; Lu, A.-Y.; Fang, W.; Lee, Y.-H.; Hsu, A. L.; Kim, S. M.; Kim, K. K.; Yang, H. Y.; Li, L.-J.; Idrobo, J.-C.; Kong, J. van der Waals Epitaxy of MoS_2 Layers Using Graphene As Growth Templates. *Nano Lett.* **2012**, *12*, 2784−2791.

(13) Zhan, Y.; Liu, Z.; Najmaei, S.; Ajayan, P. M.; Lou, J. Large-Area Vapor-Phase Growth and Characterization of MoS_2 Atomic Layers on a SiO_2 Substrate. *Small* **2012**, *8*, 966−971.

(14) Schedin, F.; Geim, A. K.; Morozov, S. V.; Hill, E. W.; Blake, P.; Katsnelson, M. I.; Novoselov, K. S. Detection of individual gas molecules adsorbed on graphene. *Nat. Mater.* **2007**, *6*, 652−655.

(15) Dan, Y.; Lu, Y.; Kybert, N. J.; Luo, Z.; Johnson, A. T. C. Intrinsic response of graphene vapor sensors. *Nano Lett.* **2009**, *9*, 1472−1475.

(16) Robinson, J. T.; Perkins, F. K.; Snow, E. S.; Wei, Z.; Sheehan, P. E. Reduced graphene oxide thin films have shown gas and vapor sensitivity. *Nano Lett.* **2008**, *8*, 3137−3140.

(17) Rumyantsev, S.; Liu, G.; Shur, M. S.; Potyrailo, R. A.; Balandin, A. A. Selective gas sensing with a single pristine graphene transistor. *Nano Lett.* **2012**, *12*, 2294−2298.

(18) Topsøe, H.; Clausen, B. S.; Massoth, F. E. *Hydrotreating Catalysis, Science and Technology*; Springer-Verlag: Berlin, 1996.

(19) Mak, K. F.; Lee, C.; Hone, J.; Shan, J.; Heinz, T. F. Atomically thin MoS_2: a new direct-gap semiconductor. *Phys. Rev. Lett.* **2010**, *105*, 136805.

(20) Splendiani, A.; Sun, L.; Zhang, Y.; Li, T.; Kim, J.; Chim, J. F. Emerging photoluminescence in monolayer MoS_2. *Nano Lett.* **2010**, *10*, 1271−1275.

(21) Li, H.; Yin, Z.; He, Q.; Li, H.; Huang, X.; Lu, G.; Fam, D. W. H.; Tok, A. Y.; Zhang, Q.; Zhang, H. Fabrication of single- and multilayer MoS_2 film-based field-effect transistors for sensing NO at room temperature. *Small* **2012**, *8*, 63−67.

(22) Snow, E. S.; Perkins, F. K.; Houser, E. J.; Badescu, S. C.; Reinecke, T. L. Chemical detection with a single-walled carbon nanotube capacitor. *Science* **2005**, *307*, 1942−1945.

(23) Snow, E. S.; Novak, J. P.; Campbell, P. M.; Park, D. Random networks of carbon nanotubes as an electronic material. *Appl. Phys. Lett.* **2003**, *82*, 2145−2147.

(24) Snow, E. S.; Perkins, F. K. Capacitance and conductance of single-walled carbon nanotubes in the presence of chemical vapors. *Nano Lett.* **2005**, *5*, 2414−2417.

(25) Alldredge, E. S.; Bădescu, Ş.C.; Bajwa, N.; Perkins, F. K.; Snow, E. S.; Reinecke, T. L.; Passmore, J. L.; Chang, Y. L. Adsorption of linear chain molecules on carbon nanotubes. *Phys. Rev. B* **2008**, *78*, 161403(R).

(26) Zonnevylle, M. C.; Hoffmann, R.; Harris, S. Thiophene hydrodesulfurization on MoS_2—theoretical aspects. *Surf. Sci.* **1988**, *199*, 320−360.

(27) Lee, C.; Yan, H.; Brus, L. E.; Heinz, T. F.; Hone, J.; Ryu, S. Anomalous Lattice Vibrations of Single- and Few-Layer MoS_2. *ACS Nano* **2010**, *4*, 2695−2700.

(28) Yaws, C. L. *Yaws' Critical Property Data for Chemical Engineers and Chemists*; Knovel, Norwich: New York, 2012.